A Source for the Continuous Generation of Pure and Quantifiable HONO Mixtures

Guillermo Villena[1] and Jörg Kleffmann[1]

[1] Department of Physical and Theoretical Chemistry, Faculty for Mathematics and Natural Sciences, University of Wuppertal, 42097 Wuppertal, Germany

Correspondence to: Jörg Kleffmann (kleffman@uni-wuppertal.de)

Abstract

A continuous source for the generation of pure HONO mixtures was developed and characterized, which is based on the Henry's law solubility of HONO in acidic aqueous solutions. With the help of a peristaltic pump diluted nitrite and sulfuric acid solutions are mixed in a temperature-controlled stripping coil, which is operated with pure nitrogen or synthetic air at gas flow rates of 0.5-2 L min^{-1}. Caused by the acidic conditions of the aqueous phase (pH $\approx$ 2.5), nitrite is almost completely converted into HONO, which partitions to the gas phase limited by its known solubility in water. The source shows a fast time response of ~2 min (0-90 %) at higher concentrations and an excellent long-time stability (2 σ noise <1 %). The HONO emission of the source perfectly correlates with the nitrite concentration from the sub-ppb range up to 500 ppb. The rate of NO_x formation increases quadratically with the HONO concentration from non-detectable values at atmospheric relevant HONO concentrations reaching a NO_x content of 1.6 % at 500 ppb. A general equation based on Henry's law is developed, whereby the HONO concentration of the source can be calculated using measured experimental parameters, i.e. nitrite concentration, liquid flow rates, gas flow rate, pH of the solution and temperature of the stripping coil. In the equation, the known Henry's law constant of HONO in sulfuric acid solutions is used. For the calculation of the effective Henry's law constant, the acid dissociation equilibrium of HONO/nitrite is used as a variable to adjust the theoretical HONO concentration to the measured values. From the average of all experimental data the equilibrium of HONO/nitrite is well described by pK_a = 1021.53/T - 0.449. The pK_a of 3.0±0.1 (1σ) at 25 °C is in good agreement with the range of 2.8-3.28 published in former studies. A standard deviation between all measured and theoretical HONO concentrations of only ±3.8 % was observed and a conservative upper limit accuracy of the HONO concentration of better 10 % is estimated. Thus, for the first time, a stable HONO source is developed, which can be used for the absolute calibration of HONO instruments.

1 Introduction

Nitrous acid (HONO) is an important trace gas in the atmosphere, which represents a major source of the OH radical (Kleffmann et al., 2005; Acker et al., 2006; Ma et al., 2013; Michoud et al., 2014; Gu et al., 2020), the detergent of the

30 atmosphere. In addition, HONO and its reaction products show mutagenic and carcinogenic properties (Pitts et al., 1978; Kirchner and Hopkins, 1991), which is especially important for indoor conditions, for which much higher levels of up to 90 ppb compared to the ambient atmosphere have been observed (Večeřa and Dasgupta, 1994).

The sources of HONO in the atmosphere are controversially discussed (Kleffmann, 2007) and among others, photochemical heterogeneous reactions have been proposed to explain unexpected high HONO concentrations during daytime (Stemmler et

35 al., 2006; Zhou et al., 2011). However, the accuracy of the daytime HONO data was often doubted, for which spectroscopic instruments are often not sensitive enough, while wet-chemical instruments may suffer from chemical interferences (Kleffmann and Wiesen, 2008). Thus, the development of sensitive and selective HONO instruments is still of high interest, for which a stable and pure HONO source is very helpful. Such a HONO source should ideally be simple in operation, produce HONO mixtures with high purity and stability, cover a wide range of concentrations and should also produce predictable

40 HONO concentrations for the calibration of HONO instruments in the field, when other calibration methods are not available. Several attempts have been made in the past to produce HONO mixtures in the laboratory and in the field. In first studies, simply the equilibrium between nitrogen oxides ($NO+NO_2$) and water vapor was used to generate HONO (Wayne and Yost, 1951):

(1) $\quad NO + NO_2 + H_2O \quad \rightleftharpoons \quad 2\ HONO$.

45 However, equilibrium (1) is never quantitative and the purity of HONO is typically lower than 50 %. Accordingly, other methods were developed, which are mainly based on different acid displacement reactions, for example using oxalic acid (Braman and de la Cantera, 1986):

(2) $\quad NaNO_2 + H_2C_2O_4 \quad \longrightarrow \quad HONO + NaHC_2O_4$,
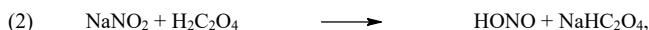
sulfuric acid (Taira and Kanda, 1990):

50 (3) $\quad NaNO_2 + H_2SO_4 \quad \longrightarrow \quad HONO + NaHSO_4$,

or hydrochloric acid (Febo et al., 1995):

(4) $\quad NaNO_2 + HCl \quad \longrightarrow \quad HONO + NaCl$.

In addition to the acid displacement, Večeřa and Dasgupta (1991) developed a source, where the thermal decomposition of ammonium nitrite was used:

55 (5) $\quad NH_4NO_2 \quad \longrightarrow \quad HONO + NH_3$.

The purity of the latter source is however low, caused by the equimolar formation of HONO and NH_3. The different types of sources used in various studies were recently summarized in Table 1 of Gingerysty and Osthoff (2020).

In most recent studies, the acid displacement using HCl was applied (Ren et al., 2010; Reed et al., 2016; Gingerysty and Osthoff, 2020; Lao et al., 2020), which are all based on the pioneering study of Febo et al. (1995). Gaseous HCl is produced

60 by any kind of permeation source and after humidification reacts heterogeneously with solid sodium nitrite. After careful optimization, high purity and a large concentration range from ppb to ppm levels can be obtained by the source (Febo et al., 1995). However, when using HCl under dry conditions or at low relative humidity, there is always a risk of undesired formation of ClNO. In addition, unreacted HCl may occur, when the sodium nitrite reactor is not working properly (Gingerysty and Osthoff, 2020). For this reason, we used this source only for a short period in our laboratory (Brust et al., 2000) and later

65 switched to the experimentally much simpler source from Taira and Kanda (1990), for which the above-mentioned by-product formation is completely absent, when using the non-volatile H_2SO_4. In the source, diluted nitrite and H_2SO_4 solutions are mixed in a temperature controlled bubbler-type reactor, while flushed with synthetic air. The HONO concentration of the

source can be adjusted simply by changing the concentration of the aqueous nitrite solution. In contrast, for the source by Febo et al. (1995), variations of the temperature and the concentration of the liquid HCl in the permeation source are required, which

70 is more complicated and time-consuming. Finally, the source of Taira and Kanda (1990) was optimized by using a temperature-controlled stripping-coil reactor, leading to even higher simplicity and stability, faster time response and to lower NO_x-formation (Kleffmann et al., 2004). The source was later commercialized (QUMA Elektronik & Analytik GmbH) and its prototype is in regular use in our laboratory and for the characterization of different HONO instruments (e.g. Jurkat et al., 2011; Ródenas et al., 2013). However, in addition to the very few information given in Kleffmann et al. (2004), the source was

75 never explained in detail. Caused by the increasing general interest in the chemistry of HONO and in the development of simple HONO sources during the last years (e.g. Gingerysty and Osthoff, 2020; Lao et al., 2020), the aim of the present study was the characterization of the source in more detail and also to apply Henry's law for its theoretical quantification to be used for the stand-alone calibration of HONO instruments.

2   Experimental

80 ### 2.1   HONO Source

The set-up of the source is shown in Figure 1. Nitrogen (N_2) from evaporation of 99.999 % pure liquid nitrogen (alternatively also synthetic air can be used) controlled by a 2 L min^{-1} flow controller (Bronckhorst) is passed through a temperature controller stripping coil (2.4 mm i.d. glass tube, 25 turns, 20 mm turn diameter) with gas flow rates in the range 0.5-2 L min^{-1}. The temperature of the stripping coil is controlled in the range 5-20 °C by a compact liquid thermostat (QUMA, Peltier type) and

85 a thermoelement, which was calibrated by a certified Hg-thermometer. The maximum temperature of the source is limited to a few °C below the dew point of water in the environment, where the source is installed, to avoid condensation of water in the PFA (perfluoroalkoxy alkanes) lines (4 mm i.d.) used. For most experiments, the source was operated at the nominal instrument set-point of 15 °C, which represents a real calibrated temperature of 15.9 °C.

In the stripping coil, the gas phase comes into contact with a mixture of diluted nitrite and H_2SO_4 solutions. Except for the

90 study of the pH dependence, a 3.6 mM H_2SO_4 solution was used, for which 2 mL of a 1/10 diluted H_2SO_4 (Aldrich p.a., 95-98 %) was diluted to 1 L with pure water. Diluted nitrite solutions (0.002-10 mg L^{-1}) were made from a 1000 mg L^{-1} standard stock solution (Merck Titrisol) by dilution with volumetric pipettes and flasks. The pH of the combined solutions of ~2.5 collected from the waste channel of the instrument was measured by a calibrated pH-meter (HANNA instruments, HI8314 membrane pH meter). The liquid flow rates of the two reagent solutions and of the waste are controlled by an 8-channel

95 peristaltic pump (Ismatec) using each 0.51 mm i.d. peristaltic pump tubing for the nitrite and H_2SO_4 solutions and a 1.14 mm i.d. tubing for the waste (Ismaprene, PharMed®), respectively. The peristaltic pump can be operated from 8-40 rpm and the liquid flow rates were measured by the time to fill 5 ml volumetric flasks. All components described above including plastic bottles for the reagents (2×0.5 L) and the waste (1 L) are installed in a 19'' rack housing (see Figure 1).
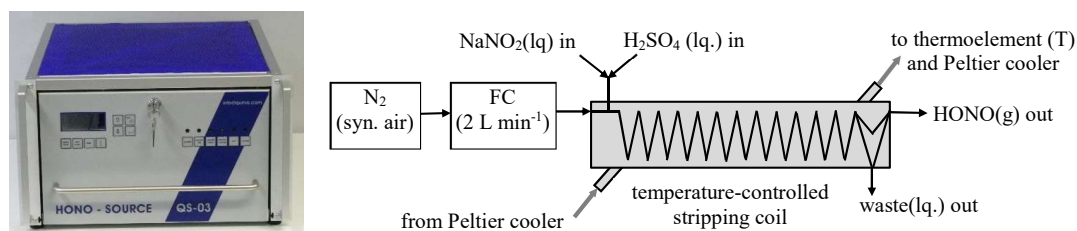
100 **Figure 1: Picture of the HONO source (QUMA) and its experimental set-up.**

2.2 Other Analytical Equipment

For the measurement of HONO and NO_x a chemiluminescence NO_x monitor (Eco-Physics, nCLD SL899) with molybdenum converter was used. The instrument has a detection limit of ~30 ppt at a sample flow rate of 1 L min^{-1} and was daily calibrated

105 by a certified NO calibration mixture (410 ppb NO, Messer) with an accuracy of 3 %. While the instrument is very selective for the detection of NO, all other reactive nitrogen species (NO_y), i.e. for the present study NO_2 and HONO, are quantitatively measured in the NO_x channel of the instrument (Villena et al., 2012). Quantitative NO_2 conversion was assured by the replacement of the molybdenum converter during the annual maintenance of the instrument just a week before the experiments and was also verified with an O_3-titration unit (Anysco GPT). Quantitative conversion of HONO to NO was demonstrated by

110 comparison with a HONO-LOPAP instrument (Heland et al., 2001; Kleffmann et al., 2002). To confirm that HONO decomposes to NO and NO_2 at equimolar ratio according to the back reaction (1) also an NO_2-LOPAP instrument (Villena et al., 2011) was used during the concentration dependency.

The HONO mixture from the source was guided by PFA-lines (4 mm i.d.) to the different instruments. The excess flow passed a humidity and temperature sensor (HYTELOG-USB, Hygrosens Instruments GmbH, accuracy ±2% RH) to measure also the

115 dewpoint of the gas phase.

3 Results

At HONO mixing ratios higher than 100 ppb significant formation of NO_x was observed (see below section 3.2), which is caused by the decomposition of HONO, see back reaction (1). In agreement with the stoichiometry of the reaction, the NO_2 concentration measured by the NO_2-LOPAP was found to be similar to the NO concentration measured by the

120 chemiluminescence instrument. Thus, for simplicity, the NO_x level of the HONO source was calculated by doubling the measured NO signal. The HONO concentration measured by the chemiluminescence monitor was then determined by the difference between $[NO_y]$ and $2\times[NO]$. The calculated HONO concentrations agreed well with those from the HONO-LOPAP in between the experimental errors of both instruments. During a concentration dependency experiment in the range 0-100 ppb (see section 3.2) both instruments showed an excellent linear correlation ($R^2 = 0.9995$) and agreement (slope LOPAP against

125 ECO: 0.972). Since the accuracy of the ECO-Physics instrument is slightly higher (3 %) than that of the HONO-LOPAP (5 %) the chemiluminescence HONO data were further used for the characterization of the HONO source.

3.1 pH Dependence

The effective solubility of HONO in aqueous solution is limited by different processes: (a) the solubility of undissociated HONO is described by Henry's law:

130 (I) $K_H = \frac{c_{lq.}}{p_g}$,

where the liquid concentration $c_{lq.}$ is given in [mol L^{-1}] and the gas phase partial pressure of HONO p_g in [atm]. In former studies consistent values of the Henry's law constant K_H [mol L^{-1} atm^{-1}] were observed (e.g. Park and Lee, 1988; Becker et al., 1996).

(b) since H_2SO_4 solutions were used in the present study, the salting out effect of the weak acid HONO by the strong acid

135 H_2SO_4 has to be considered. Thus, for the HONO/H_2SO_4 system the solubility data from our former study Becker et al. (1996) was used, which agreed well with the results from Park and Lee (1988) for pure water.

(c) considering that only a moderate acidity of the reaction mixture was finally used (pH $\approx$ 2.5, see below), the added nitrite is still not completely converted into undissociated HONO in the aqueous phase, caused by the pH-dependent acid dissociation equilibrium:

140 (6)   HONO $\rightleftharpoons$ $NO_2^- + H^+$.

To quantitatively describe the equilibrium (6), pK_a values in the range 2.8-3.26 have been published in former studies (Park and Lee, 1988; Riordan et al., 2005; da Silva et al., 2006). Considering this equilibrium, the effective Henry's law constant $K_{H,eff.}$ [mol L^{-1} atm^{-1}] is given by:

(II) $K_{H,eff.} = K_H \left(1 + \frac{K_a}{[H^+]}\right),$

145   where the H$^+$ concentration [mol L^{-1}] is calculated from the measured pH of the combined solutions (waste). Since the acid dissociation constant has a significant uncertainty, we used the pK_a as unknown variable to adjust the theoretical HONO concentrations (see equation (III), section 4.2) to the experimental values. When using all experimental data at pH >2.4 and excluding the temperature dependence, an average pK_a = 3.09±0.12 (1σ) was determined at the typical used temperature of 15.9 °C. When the temperature dependence was also considered (see section 3.5) the equilibrium is well described by pK_a =

150   1021.53/T - 0.449 in the experimental temperature range (5.4-18.6 °C). The resulting pK_a of 3.0±0.1 (1σ) at 25 °C is in good agreement with the range of 2.8-3.28 published in former studies (Park and Lee, 1988; Riordan et al., 2005; da Silva et al., 2006).

When the pH of the solution was varied, an excellent agreement between theoretical (see section 4.2) and experimental HONO concentrations was observed only for pH values >2.4. For lower pH significantly lower HONO concentrations were observed

155   in comparison with the values calculated with equation (III) (see Figure 2). Reasons for this discrepancy are still unclear and could not be explained by the increasing rate of NO_x formation with decreasing pH, as even the measured NO_y concentration was lower than the theoretical HONO concentration (see Figure 2). One potential problem could be the pH measurements, which showed excellent agreement between measured and theoretical values (considering the acid concentration and assuming quantitative dissociation of H_2SO_4) only for pH >2, but significantly larger values at high acidity (Bates, 1973). Since

160   quantitative dissociation of the strong H_2SO_4 can be assumed down to pH = 0, the theoretical and not the experimental pH-values were used for pH <2 in Figure 2. Furthermore, according to the study by Riordan et al. (2005) a second equilibrium between $HONO_{aq.}$ and $H_2ONO^+_{aq.}$ at pH <2 could lead to a higher effective solubility compared to undissociated HONO. However, in our former study Becker et al. (1996), the equilibrium between HONO and NO^+ was observed at much higher acidity around 55 wt%, which was in good agreement with a former study by Seel and Winkler (1960). Thus, any increasing

165   effective solubility by formation of H_2ONO^+/NO^+ should not be of importance in the pH range 0-2. Finally, liquid phase diffusion in the stripping coil could limit the experimental HONO emission with increasing viscosity of the H_2SO_4 solutions at concentrations up to 2.7 wt% used, leading to lower HONO concentrations than theoretically expected from the thermodynamic equilibrium. In contrast, in our study by Becker et al. (1996) on which equation (III) is based, a bubbler set-up was used under thermodynamic equilibrium.

170   Since our focus was not the exact study of the system N(III) in sulfuric acid solutions, but the development of a HONO source, we not further investigated this issue in detail, but simply limited the acidity to pH ≥2.4. For these conditions, a) the pH-measurements were accurate, b) the theoretical and experimental HONO concentrations agreed well, c) a potential equilibrium of HONO and H_2ONO^+ is still not significant (Riordan et al., 2005) and d) the unwanted NO_x formation is still small (see Figure 2). The pH should however also not be too high (i.e. >3), since the uncertainties in the theoretical HONO concentrations

175   increase at higher pH, caused by the incomplete conversion of the added nitrite to HONO, see equilibrium (6). Thus, for the present HONO source an acidity of the reaction mixture of pH ≈ 2.5 is recommended.
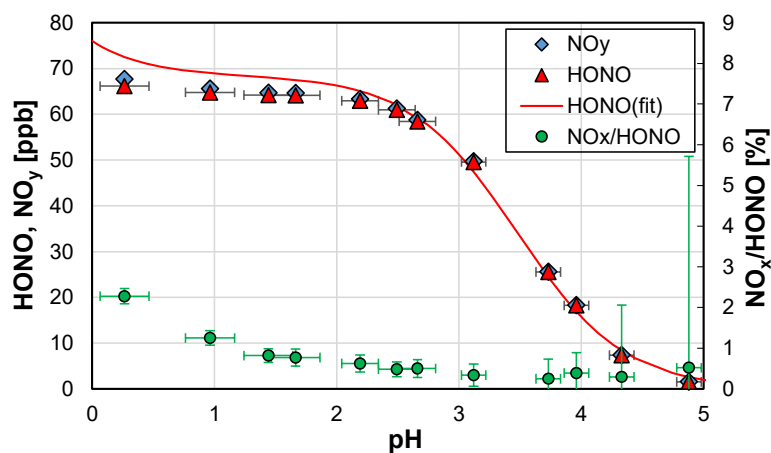
Figure 2: Dependence of the HONO mixing ratio and the ratio NOₓ/HONO on the pH of the NO₂⁻/H₂SO₄ reaction mixture (NO₂⁻ =
180   1 mg L⁻¹; T = 15.9 °C, $\phi^0_{g,dry}$ = 1570 cm³ min⁻¹, 20 rpm). In addition, the theoretical HONO mixing ratios calculated by equation
(III), see section 4.2, are also shown, for which a pK_a = 3.16 was used (weighted average of all shown data at pH >2.4).

3.2   Concentration Dependence

The dependence of the added nitrite concentration on the HONO mixing ratio was studied in two different experiments and by
185   two different operators of the source. The experimental data from one experiment is shown in Figure 3, for which the nitrite
concentration was varied by several orders of magnitude (0.002 – 10 mg L⁻¹). The source showed a very fast time response of
~2 min (0-90 %) for HONO concentrations >20 ppb increasing to 6-7 min at lower concentrations at a liquid pump speed of
20 rpm.

When all HONO data from the two experiments were plotted against the nitrite concentration an excellent linear correlation
190   (R^2 = 0.99996) was observed. Similar slopes were observed when using all HONO data up to 500 ppb (see Figure 4 A)
compared to mixing ratios only up to 10 ppb (see Figure 4 B). At typical atmospheric HONO mixing ratios <20 ppb no NOₓ
formation was observed in between the experimental errors. Only at higher HONO levels, NOₓ quadratically increased with
the HONO concentration (see Figure 4 A), in agreement with the expected second order kinetic behaviour of the back reaction
(1). But even at 500 ppb HONO, a NOₓ content of only 1.6 % was observed, which is significantly lower than in the original
195   bubbler set-up of Taira and Kanda (1990). Thus, the HONO source can be operated for mixing ratios up to 500 ppb and up to
20 ppb with purities of >98 % and >99.8 %, respectively. In addition, the excellent agreement of the HONO and NOₓ data for
the two completely independent experiments performed by two different operators including different NOₓ calibration and
dilution of the nitrite stock solution (see Figure 4) demonstrates the high precision and reproducibility of the HONO source
(see also section 3.6).
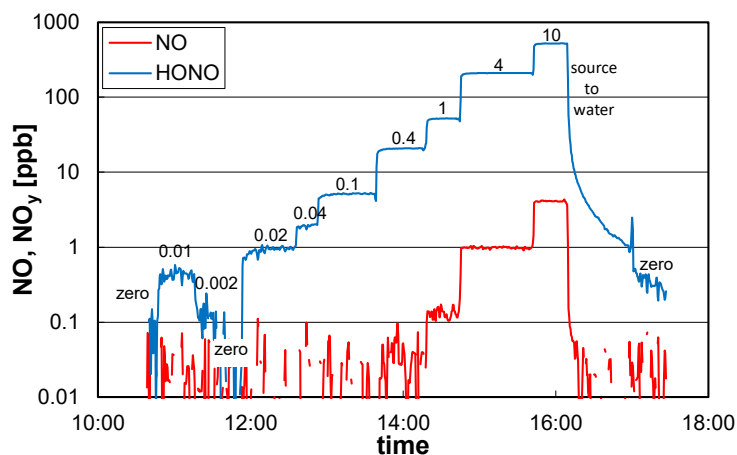
200

Figure 3: NO and HONO concentrations of the HONO source (logarithmic scale) for variable nitrite concentrations (numbers in the figure in mg L^{-1}). The HONO signal of the chemiluminescence instrument shows significant tailing for zero measurements, which follow high HONO concentrations (see last zero). Experimental conditions: T = 15.9 °C, $\phi_{g,dry}^{\emptyset}$ = 2104 cm^3 min^{-1}, 20 rpm, pH = 2.48.
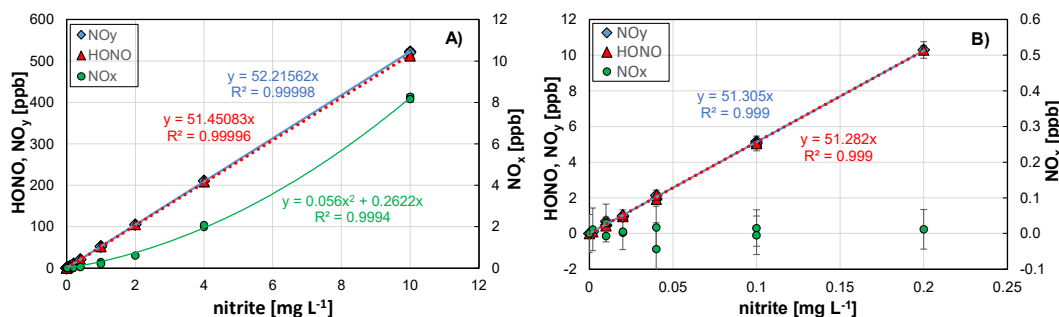
205

Figure 4: Nitrite-concentration dependence of the NO$_y$, HONO and NO$_x$ formation of the HONO source for two independent experiments. A) All data including the data shown in Figure 3; B) same data for nitrite concentrations ≤0.2 mg L^{-1} (T = 15.9 °C, $\phi_{g,dry}^{\emptyset}$ = 2104 cm^3 min^{-1}, 20 rpm, pH = 2.45 and 2.48).

3.3 Gas Flow Rate Dependence

210 The used stripping coil can be operated at gas flow rates in the range 0.5-2 L min^{-1}. However, caused by the sample flow rate of the chemiluminescence instrument of 1 L min^{-1}, only gas flow rates in the range 1-2 L min^{-1} were investigated. The HONO concentration was decreasing with the gas flow rate (see Figure 5), which can be explained by the increasing dilution of the formed HONO in the increasing gas volume.

Furthermore, a decreasing NO$_x$ content with increasing gas flow rate was observed, which is explained by the decreasing

215 reaction time of HONO in the stripping coil and the heterogeneous decomposition of HONO (back reaction (1), second order kinetics). Thus, for increasing the purity of the source, it should be operated at gas flow rates >1.5 L min^{-1}. If lower flow rates are necessary, the HONO levels should be reduced to mixing ratios <10 ppb, caused by the quadratic dependence of the NO$_x$ formation with the HONO mixing ratio, see section 3.2. The time response of the source was found to be independent of the gas flow rate.
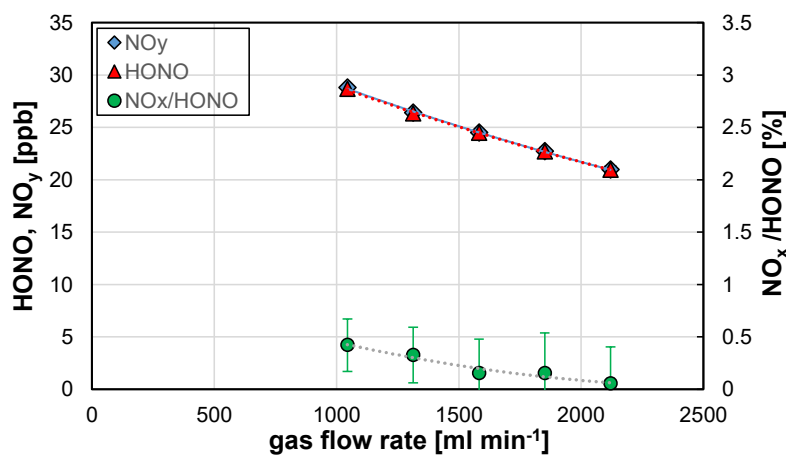
220

Figure 5: Gas flow rate dependence of NO$_y$, HONO and the ratio NO$_x$/HONO of the HONO source (NO$_2^-$ = 0.4 mg L^{-1}, T = 15.9 °C, 20 rpm, pH = 2.47).

3.4 Liquid Flow Dependence

225 Since the amount of nitrite pumped into the stripping coil is directly proportional to the liquid flow rate, the speed of the liquid peristaltic pump was varied in the range 10-40 rpm. As expected, the HONO mixing ratios increased with the liquid flow rate (see Figure 6). However, the increase was found to be non-linear, since at higher liquid flow rates the liquid volume in the stripping coil is also increasing. Thus, an increasing content of nitrite/HONO is remaining in the liquid phase according to Henry's law.

230 No significant impact of the NO$_x$ formation on the liquid flow was observed (see Figure 6). This could be explained by the heterogeneous back reaction (1) that only occurs on the surface of the stripping coil, which is not affected by the liquid flow rate. In contrast, if the decomposition of HONO proceeded via a liquid phase reaction, NO$_x$ formation should increase with the liquid flow rate. As expected, the time response of the source was observed to decrease with the liquid flow rate, which can be explained by faster liquid exchange in the stripping coil.
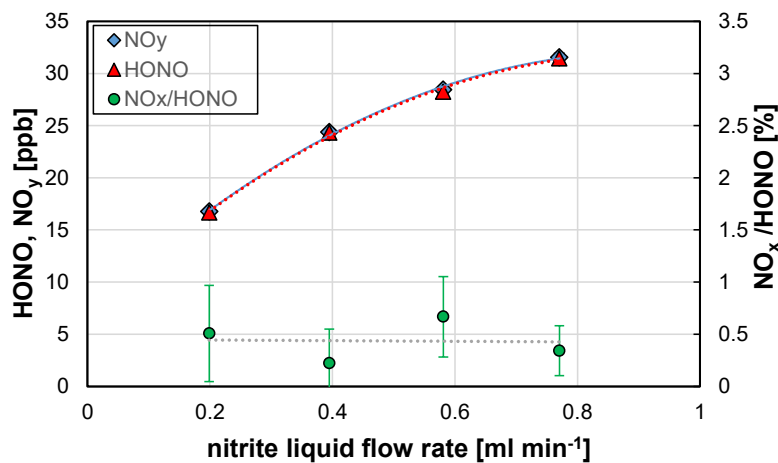
235

Figure 6: Nitrite liquid flow rate dependence (10, 20, 30, 40 rpm of the peristaltic pump) of NO$_y$, HONO and the ratio NO$_x$/HONO of the HONO source (NO$_2^-$ = 0.4 mg L^{-1}, T = 15.9 °C, $\phi^0_{g,dry}$ = 1570 cm^3 min^{-1}, pH = 2.47).

3.5 Temperature Dependence

240 Since the solubility of HONO is temperature dependent (Park and Lee, 1988), also the temperature of the stripping coil was
varied in the range 5.4-18.6 °C. The maximum temperature of the stripping coil is limited to a few degrees below the laboratory
temperature, to exclude condensation of water on surfaces behind the stripping coil. Here, strong fluctuation of the HONO
concentration was observed when the source was operated close to the dewpoint of water. The lower temperature limit is given
by the power of the Peltier cooler of the source. Besides the HONO levels, also the humidity of the gas phase can be varied by
245 the temperature of the stripping coil.

As expected from the known solubility data (Park and Lee, 1988; Becker et al., 1996), the HONO concentration of the source
was found to increase with the temperature (see Figure 7). In contrast, the NO_x content of the source was slightly decreasing
with the temperature, which was not caused by decreasing absolute NO_x concentrations, but by the increasing HONO levels.
Similar to the other experiments, the theoretical HONO concentrations calculated by equation (III) (see section 4.2) were
250 adjusted to the measured values by varying the pK_a for the acid dissociation equilibrium (6), leading to a decreasing pK_a with
increasing temperature; for the quantitative description, see section 3.1.
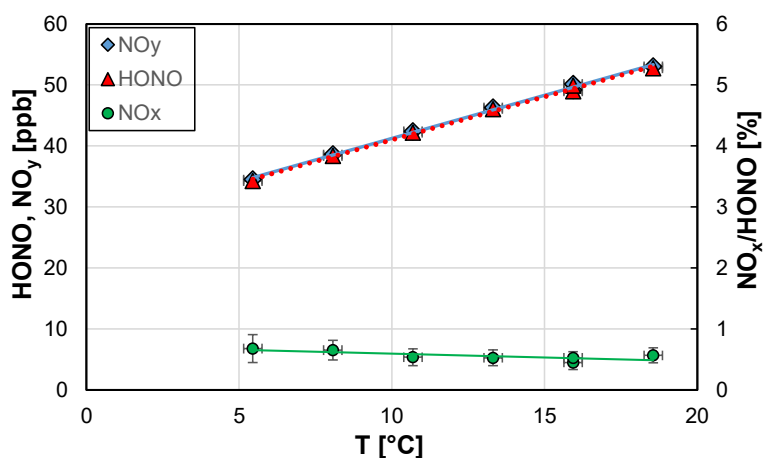
Figure 7: Temperature dependence of NO_y, HONO and the ratio NO_x/HONO of the HONO source ($NO_2^- = 0.8$ mg L^{-1}, $\phi^0_{g,dry} = 1570$
cm^3 min^{-1}, 20 rpm, pH = 2.46).

255

3.6 Stability Test

To test the long-term stability and precision, the source was operated overnight at constant experimental conditions at a low
liquid pump speed of 10 rpm leading to reduced liquid consumption and a time response (0-90 %) of the source of ~4 min.
The final HONO concentration varied by <1 % (2σ noise: 0.76 %), see Figure 8. This high precision is similar to the precision
260 of the chemiluminescence instrument used to quantify the HONO source. Thus, the given precision error of the source is even
an upper limit.

With the reduced liquid flow rate and using the internal liquid containers of the instrument, the source can be continuously
operated for ~43 hours. If longer operation is necessary 5 L (nitrite, H$_2$SO$_4$) and 10 L (waste) liquid bags could be used.
However, for such long periods the liquid flow rate of a peristaltic pump is typically slightly decreasing with time, leading to
265 some expected drift of the HONO source. In this case, the liquid flow rates (nitrite, waste) should be regularly measured and
included in the calculation of the theoretical HONO concentration, see section 4.2.
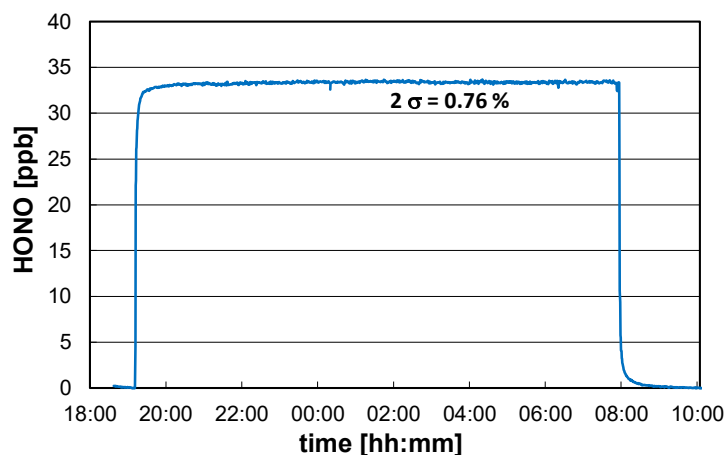
Figure 8: Stability test of the HONO source (NO_2^- = 0.8 mg L^{-1}, T = 15.9 °C, $\phi_{g,dry}^0$= 1570 cm^3 min^{-1}, 10 rpm, pH = 2.47).

4   Discussion

4.1   General Considerations

270   A HONO source was developed and characterized, where HONO is produced by the reaction of diluted nitrite and H_2SO_4 solutions in a temperature-controlled stripping coil. The advantage of using H_2SO_4 is the missing formation of unwanted by-products like HCl and ClNO as observed in HONO sources using the volatile HCl, which are based on the original concept of Febo et al. (1995). While these sources can be carefully optimized for low by-product formation (Febo et al., 1995; Gingerysty

275   and Oshoff, 2020; Lao et al., 2020), the use of the non-volatile H_2SO_4 completely excludes the still existing risk of any malfunction of the source. For example, when the Febo et al. source was used in our laboratory two decades ago (Brust et al., 2000), we often had problems related with the homogeneous mixing of the solid $NaNO_2$ and with the use of low relative humidity, leading to lower purity of HONO.

Further advantages of the new HONO source are:

280   a)   The high time response (0-90%) of 1.5-7 min depending on the liquid flow rates and the HONO concentration levels used. For a typical pump speed of 20 rpm and HONO levels >20 ppb a time response of 2 min was observed. In contrast, the sources of Taira and Kanda (1990) and Febo et al. (1995) show much longer time responses. Even when the original source from Febo et al. (1995) was optimized by using a modified HCl permeation source and a solid $NaNO_2$ coated flow tube reactor, HONO stabilisation times of several hours were observed, even when the HCl permeation source was running

285   constantly (Lao et al., 2020). Furthermore, for the HCl permeation source stabilization times of a week and more were necessary, still leading to some unwanted peaks of the permeation rate after this long stabilization time (Lao et al., 2020). In contrast, the present HONO source can be started under water, which can additionally be used to zero any HONO instrument and after 1 h stabilisation of the liquid flow rate of the peristaltic pump stable HONO concentrations are obtained in a few minutes, when water is exchanged by the nitrite and H_2SO_4 reagents.

290   b)   The wide mixing ratio range of 0.1-500 ppb, simply by changing the nitrite concentration. Here, a very linear correlation between HONO and nitrite is observed. Different concentrated nitrite solutions can be easily made with high accuracy by dilution of a stock solution using volumetric pipettes and flasks. In contrast, for the source of Febo et al. (1995), different concentrated HCl solutions and HCl temperatures have to be used to adjust the output of the source, which is much more difficult and time-consuming.

295   c) The high purity of the source. For HONO mixing ratios <20 ppb no NO_x formation and a purity of >99.8 % is observed. And even at high HONO levels of 500 ppb the purity of the source is >98 %. In contrast, for other recent HONO sources only purities >95 % and >90% were observed, respectively (Gingerysty and Osthoff, 2020; Lao et al., 2020).

   d) The high long-term stability and precision of the source. After stabilisation, an upper limit 2σ precision of the source of 0.76 % was observed, which is similar to the precision error of the used NO_x instrument.

300   e) The wide variability of the experimental conditions. Here, the liquid and gas flow rates and the temperature can be varied, leading for example, to variable humidity, time response and reagent consumption of the source.

   f) The predictability of the HONO output. The absolute HONO concentration can be calculated based on Henry's law with high accuracy (see next section 4.2), which offers for the first time the possibility of using a HONO source for the absolute calibration of HONO instruments.

305   **4.2   Theoretical Calculation of the HONO Concentration**

When the acidity of the reaction mixture was fixed to pH $\approx$ 2.5, for which the effective solubility of HONO is well described by the Henry's law solubility and the acid dissociation equilibrium (6), see section 3.1, the experimental HONO mixing ratios of the source are calculated by equation (III):

(III) $[HONO]_{theo.} = \dfrac{c_{NO_2^-} \cdot \phi_{NO_2^-} \cdot N_A}{M_{NO_2^-} \cdot \left(N_A \cdot \phi_{waste} \cdot K_{H_{eff}} \cdot p + \frac{N^{p,T}}{V} \cdot \phi_g^{p,T,r.h.} \right)} \cdot 10^{-9}$ [ppb],

310   where $c_{NO_2^-}$ represents the nitrite concentration [g L^{-1}], $\phi_{NO_2^-}$ the nitrite liquid flow rate (L min^{-1}), N_A the Avogadro constant ($6.02214 \cdot 10^{23}$ molecules mol^{-1}), $M_{NO_2^-}$ the molar mass of nitrite (46.005 g mol^{-1}), ϕ_{waste} the liquid flow rate of the waste (L min^{-1}), $K_{H_{eff}}$ the effective Henry's law constant (mol L^{-1} atm^{-1}, see section 3.1), p the ambient pressure (atm), $\frac{N^{p,T}}{V}$ the number density of the gas phase according to the ideal gas law at ambient pressure and temperature of the stripping coil (molecules cm^{-3}) and $\phi_g^{p,T,r.h.}$ the gas flow rate at ambient pressure, temperature of the stripping coil and considering the evaporation of

315   water at the temperature of the stripping coil (cm^3 min^{-1}). $\phi_g^{p,T,r.h.}$ is calculated by:

(IV) $\phi_g^{p,T,r.h.} = \phi_g^{\emptyset,dry} \cdot \dfrac{T^{exp.}}{T^{\emptyset}} \cdot \dfrac{p^{\emptyset}}{p^{exp.}} \cdot \dfrac{p^{exp.}}{(p^{exp.} - p^{water})}$,

where $\phi_g^{\emptyset,dry}$ is the gas flow rate (cm^3 min^{-1}) of the calibrated flow controller at dry standard conditions ($T^{\emptyset} = 298.15$ K, $p^{\emptyset} = 1$ atm) and $T^{exp.}$ and $p^{exp.}$ the experimental temperature (K) and pressure (atm), respectively. To calculated the water vapor pressure p^{wate} (atm) the Magnus equation was used (Alduchov and Eskridge, 1996):

320   (V) $p^{water} = 6.1094 \cdot exp\left(\dfrac{17.625 \cdot t(°C)}{243.04 + t(°C)} \right) \cdot \dfrac{1}{1013.25}$.

The measured liquid flow rate of the waste ϕ_{waste} was in excellent agreement with the sum of the flow rates of nitrite and H_2SO_4 considering the theoretical water evaporation in the stripping coil, confirming an almost complete saturation of the gas phase by water vapor at the temperature of the stripping coil. The liquid flow rates were measured by the time taken to fill up 5 ml volumetric flasks.

325   When all experimental data described in the previous sections, excluding the pH dependence (see section 3.1), were compared to the theoretical HONO concentrations, a weighted average ratio $[HONO]_{exp.}/[HONO]_{theo.}$ of 0.996 was observed. This excellent agreement is trivial, since the applied pK_a was derived from the average of all individual adjusted values for fitting the theoretical HONO mixing ratios to the measured values, see section 3.1. However, more importantly, the average 1σ standard deviation of all $[HONO]_{exp.}/[HONO]_{theo.}$ ratios was only 3.8 %, despite the high variability of the experimental

330   conditions applied. When the less precise data at [HONO] <5 ppb were excluded, the average 1σ standard deviation of the $[HONO]_{exp.}/[HONO]_{theo.}$ ratios was even only 1.7 %, showing the very high precision of the source.

Besides this high precision, also a high accuracy of better than 10 % is estimated for the HONO source, which is mainly based on the accuracy of the used chemiluminescence monitor (3 %), the precision error of all data for HONO concentrations >5 ppb (1.7 %) and the errors in the different variables used in equation (III). For the liquid nitrite concentration an accuracy of

335 typically 3-4 % is obtained, considering the accuracy of the nitrite stock solution of 1000 mg L^{-1} (1 %) and those of the used volumetric pipettes and flasks. An accuracy of 2 % is estimated for the gas flow rate, since the flow controller was used at 50-100 % of its nominal flow rate. In addition, it was calibrated during the experiments with a soap bubble flow tube, for which temperature, pressure and water evaporation were carefully considered. Accuracies of the liquid flow rates of 1 % are estimated. The error of the theoretical HONO concentration induced by the pH-measurements is estimated to 1.5 %. And

340 finally, the error introduced by the uncertainty of the stripping coil temperature of ±0.5 °C is 1 %. By error propagation a combined accuracy of ±5.8 % is obtained.

Because of the accuracy of better than 10 %, the HONO source can be used as a stand-alone device to absolutely calibrate HONO instruments, for which no simple calibration is available, e.g. mass spectrometers. In contrast, instruments which measure HONO after sampling in a liquid phase (HPLC, WEDD, LOPAP, etc.) can typically be calibrated by using liquid

345 nitrite standards. However, even these instruments need careful characterization, for example of the sampling and detection efficiencies, where a pure HONO source would be also very helpful. And finally, the HONO source can be used to study the chemistry of HONO in the laboratory.

5   Conclusion

In the present study, a HONO source is developed and characterized, which is based on the effective Henry's law solubility of

350 HONO in water. Diluted nitrite and sulfuric acid solutions are mixed in a temperature-controlled stripping coil, which is operated with pure nitrogen or synthetic air at gas flow rates of 0.5-2 L min^{-1}. Under the acidic conditions of the combined reaction mixture (pH ≈ 2.5), nitrite is almost completely converted into HONO, which partitions to the gas phase. The known Henry's law constant of HONO in H_2SO_4 is used for the calculation of the effective solubility. In addition, in the present study the acid dissociation equilibrium is described by pK_a = 1021.53/T - 0.449. The pK_a of 3.0±0.1 (1σ) at 25 °C is in good

355 agreement with the range of 2.8-3.28 published in former studies. The source shows a fast time response of ~2 min (0-90 %) at higher concentrations and an excellent long-time stability (2 σ noise 0.76 %). The HONO emission of the source perfectly correlates with the nitrite concentration from the sub-ppb range up to 500 ppb. The rate of NO_x formation increases quadratically with the HONO concentration from non-detectable values at atmospheric relevant HONO concentrations reaching a NO_x content of 1.6 % at 500 ppb. A general equation based on the effective Henry's law solubility is developed, by

360 which the HONO concentration of the source can be calculated using measured experimental parameters, i.e. nitrite concentration, liquid flow rates, gas flow rate, pH of the solution and temperature of the stripping coil. An average deviation between measured and theoretical HONO concentration of only ±3.8 % is observed and a conservative accuracy of the calculated HONO concentration of better 10 % is estimated. Thus, for the first time, a HONO source is developed, which can be used for the absolute calibration of HONO instruments.

365   6   Acknowledgement

7   References

Acker, K., Möller, D., Wieprecht, W., Meixner, F. X., Bohn, B., Gilge, S., Plass-Dülmer, C., and Berresheim, H.: Strong Daytime Production of OH from HNO$_2$ at a Rural Mountain Site, Geophys. Res. Lett., 33(2), L02809, doi: 10.1029/2005GL024643, 2006.

370   Alduchov, O. A., and Eskridge, R. E.: Improved Magnus Form Approximation of Saturation Vapor Pressure, J. Appl.
        Meteorol., 35, 601-609, doi: 10.1175/1520-0450(1996)035<0601:IMFAOS>2.0.CO;2, 1996.

        Bates, R. G.: Determination of pH, Theory and Practice, John Wiley & Sons, New York, ISBN 0-471-05647-2, 1973.

        Becker, K. H., Kleffmann, J., Kurtenbach, R., and Wiesen, P.: Solubility of Nitrous Acid (HONO) in Sulfuric Acid Solutions,
        J. Phys. Chem., 100, 14984-14990, doi: 10.1021/jp961140r, 1996.

375   Braman, R. S., and de la Cantera, M. A.: Sublimation Source for Nitrous Acid and Other Nitrogen Compounds in Air, Anal.
        Chem., 58, 1533-1537, doi: 10.1021/ac00298a059, 1986.

        Brust, A. S., Becker, K. H., Kleffmann, J., and Wiesen, P.: UV Absorption Cross Sections of Nitrous Acid, Atmos. Environ.,
        34, 13-19, doi: 10.1016/S1352-2310(99)00322-2, 2000.

        da Silva, G., Kennedy, E. M., and Dlugogorski, B. Z.: Ab Initio Procedure for Aqueous-Phase pK_a Calculation: The Acidity
380   of Nitrous Acid, J. Phys. Chem. A, 110(39), 11371-11376, doi: 10/1021/jp0639243, 2006.

        Febo, A., Perrino, C., Gherardi, M., and Sparapani, R.: Evaluation of a High-Purity and High-Stability Continuous Generation
        System for Nitrous Acid, Environ. Sci. Technol., 29(9), 2390-2395, doi: 10.1021/es00009a035, 1995.

        Gingerysty, N. J. and Osthoff, H. D.: A compact, high-purity source of HONO validated by Fourier transform infrared and
        thermal-dissociation cavity ring-down spectroscopy, Atmos. Meas. Tech., 13, 4159-4167, doi: 10.5194/amt-13-4159-2020,
385   2020.

        Gu, R., Zheng, P., Chen, T., Dong, C., Wang, Y., Liu, Y., Liu, Y., Luo, Y., Han, G., Wang, X., Zhou, X., Wang, T., Wang,
        W., and Xue, L.: Atmospheric Nitrous Acid (HONO) at a Rural Coastal Site in North China: Seasonal Variations and Effects
        of Biomass Burning, Atmos. Environ., 229, 117429, doi: 10.1016/j.atmosenv.2020.117429, 2020.

        Heland, J., Kleffmann, J., Kurtenbach, R., and Wiesen, P.: A New Instrument to Measure Gaseous Nitrous Acid (HONO) in
390   the Atmosphere, Environ. Sci. Technol., 35(15), 3207-3212, doi: 10.1021/es000303t, 2001.

        Jurkat, T., Voigt, C., Arnold, F., Schlager, H., Kleffmann, J., Aufmhoff, H., Schäuble, D., Schaefer, M., and Schumann, U.:
        Measurements of HONO, NO, NO_y and SO_2 in aircraft exhaust plumes at cruise, Geophys. Res. Lett., 38, L10807, doi:
        10.1029/2011GL046884, 2011.

        Kirchner, J. J., and Hopkins, P. B.: Nitrous Acid Cross-Links Duplex DNA Fragments through Deoxyguanosine Residues at
395   the Sequence 5´-CG, J. Am. Chem. Soc., 113, 4681-4682, doi: 10.1021/ja00012a047, 1991.

        Kleffmann, J., Heland, J., Kurtenbach, R., Lörzer, J., and Wiesen, P.: A New Instrument (LOPAP) for the Detection of Nitrous
        Acid (HONO), Environ. Sci. Pollut. Res., 9 (special issue 4), 48-54, 2002.

        Kleffmann, J., Benter, T., and Wiesen, P.: Heterogeneous Reaction of Nitric Acid with Nitric Oxide on Glass Surfaces under
        Simulated Atmospheric Conditions, J. Phys. Chem. A, 108(27), 5793-5799, doi: 10.1021/jp040184u, 2004.

400   Kleffmann, J., Gavriloaiei, T., Hofzumahaus, A., Holland, F., Koppmann, R., Rupp, L., Schlosser, E., Siese, M., and Wahner,
        A.: Daytime Formation of Nitrous Acid: A Major Source of OH Radicals in a Forest, Geophys. Res. Lett., 32(5), L05818,
        doi:10.1029/2005GL022524, 2005.

        Kleffmann, J.: Daytime Sources of Nitrous Acid (HONO) in the Atmospheric Boundary Layer, Chem. Phys. Chem., 8(8),
        1137-1144, doi: 10.1002/cphc.200700016, 2007.

405   Kleffmann, J., and Wiesen, P.: Technical Note: Quantification of Interferences of Wet Chemical HONO LOPAP
        Measurements under Simulated Polar Conditions, Atmos. Chem. Phys., 8(22), 6813–6822, doi: 10.5194/acp-8-6813-2008,
        2008.

        Lao, M., Crilley, L. R., Salehpoor, L., Furlani, T. C., Bourgeois, I., Neuman, J. A., Rollins, A. W., Veres, P. R., Washenfelder,
        R. A., Womack, C. C., Young, C. J., and VandenBoer, T. C.: A portable, robust, stable, and tunable calibration source for gas-
410   phase nitrous acid (HONO), Atmos. Meas. Tech., 13, 5873-5890, doi: 10.5194/amt-13-5873-2020, 2020.

Ma, J., Liu, Y., Han, C., Ma, Q., Liu, C., and He, H.: Review of heterogeneous photochemical reactions of NO_y on aerosol - A possible daytime source of nitrous acid (HONO) in the atmosphere, J. Environ. Sci., 25(2), 326-334, doi: 10.1016/S1001-0742(12)60093-X, 2013.

Michoud, V., Colomb, A., Borbon, A., Miet, K., Beekmann, M., Camredon, M., Aumont, B., Perrier, S., Zapf, P., Siour, G.,
415 Ait-Helal, W., Afif, C., Kukui, A., Furger, M., Dupont, J. C., Haeffelin, M., and Doussin, J. F.: Study of the unknown HONO daytime source at a European suburban site during the MEGAPOLI summer and winter field campaigns, Atmos. Chem. Phys., 14, 2805-2822, doi: 10.5194/acp-14-2805-2014, 2014.

Park, J.-Y., and Lee, Y.-N.: Solubility and Decomposition Kinetics of Nitrous Acid in Aqueous Solution, J. Phys. Chem., 92, 6294-6302, doi: 10.1021/j100333a025, 1988.

420 Pitts Jr., J. N., Grosjean, D., Van Cauwenberghe, K., Schmid, J. P., and Fitz, D. R.: Photooxidation of Aliphatic Amines under Simulated Atmospheric Conditions: Formation of Nitrosamines, Nitramines, Amides, and Photochemical Oxidant, Environ. Sci. Technol., 12(8), 946-953, doi: 10.1021/es60144a009, 1978.

Reed, C., Brumby, C. A., Crilley, L. R., Kramer, L. J., Bloss, W. J., Seakins, P. W., Lee, J. D. and Carpenter, L. J.: HONO measurement by differential photolysis, Atmos. Meas. Tech., 9, 2483-2495, doi: 10.5194/amt-9-2483-2016, 2016.

425 Ren, X., Gao, H., Zhou, X., Crounse, J. D., Wennberg, P. O., Browne, E. C., LaFranchi, B. W., Cohen, R. C., McKay, M., Goldstein, A. H., and Mao, J.: Measurement of Atmospheric Nitrous Acid at Bodgett Forest during BEARPEX2007, Atmos. Chem. Phys., 10, 6283-6294, doi: 10.5194/acp-10-6283-2010, 2010.

Riordan, E., Minogue, N., Healy, D., O'Driscoll, P., and Sodeau, J. R.: Spectroscopic and Optimization Modeling Study of Nitrous Acid in Aqueous Solution, J. Phys. Chem. A, 109(5), 779-786, doi: 10.1021/jp040269v, 2005.

430 Ródenas, M., Muñoz, A., Alacreu, F., Brauers, T., Dorn, H.-P., Kleffmann, J., and Bloss, W. J.: Assessment of HONO Measurements: The FIONA Campaign at EUPHORE. In: Barnes, I., Rudziński, K. (eds), Disposal of Dangerous Chemicals in Urban Areas and Mega Cities. Role of Oxides and Acids of Nitrogen in Atmospheric Chemistry. NATO Science for Peace and Security Series C: Environmental Security. Springer, Dordrecht, 45-58, doi: 10.1007/978-94-007-5034-0_4, 2013.

Seel, F., and Winkler, R.: Das Gleichgewicht salpetrige Säure–Stickoxydkation im System Schwefelsäure–Wasser, Z. Phys.
435 Chem., 25, 217-232, doi: 10.1524/zpch.1960.25.3_4.217, 1960.

Stemmler, K., Ammann, M., Donders, C., Kleffmann, J., and George, C.: Photosensitized Reduction of Nitrogen Dioxide on Humic Acid as a Source of Nitrous Acid, Nature, 440(7081), 195-198, doi: 10.1038/nature04603, 2006.

Taira, M., and Kanda, Y.: Continuous Generation System for Low-Concentration Gaseous Nitrous Acid, Anal. Chem., 62(6), 630-633, doi: 10.1021/ac00205a018, 1990.

440 Večeřa Z., and Dasgupta, P. K.: Measurement of Ambient Nitrous Acid and a Reliable Calibration Source for Gaseous Nitrous Acid, Environ. Sci. Technol., 25, 255-260, doi: 10.1021/es00014a006, 1991.

Večeřa, Z., and Dasgupta, P. K.: Indoor Nitrous Acid Levels. Production of Nitrous Acid from Open-Flame Sources, Int. J. Environ. Anal. Chem., 56(4), 311-316, doi: 10.1080/03067319408034109, 1994.

Villena, G., Bejan, I., Kurtenbach, R., Wiesen, P., and Kleffmann, J.: Development of a new Long Path Absorption Photometer
445 (LOPAP) Instrument for the Sensitive Detection of NO_2 in the Atmosphere, Atmos. Meas. Tech., 4, 1663-1676 doi: 10.5194/amt-4-1663-2011, 2011.

Villena, G., Bejan, I., Kurtenbach, R., Wiesen, P., and Kleffmann, J.: Interferences of commercial NO_2 instruments in the urban atmosphere and in a smog chamber, Atmos. Meas. Tech., 5, 149-159, doi: 10.5194/amt-5-149-2012, 2012.

Wayne, L. G., and Yost, D. M.: Kinetics of the Rapid Gas Phase Reaction between NO, NO_2, and H_2O, J. Chem. Phys., 19(1),
450 41-47, doi: 10.1063/1.1747986, 1951.

Zhou, X., Zhang, N., TerAvest, M., Tang, D., Hou, J., Bertman, S., Alaghmand, M., Shepson, P. B., Caroll, M. A., Griffith, S., Dusanter, S., and Stevens, P. S.: Nitric Acid Photolysis on Forest Canopy Surface as a Source for Tropospheric Nitrous Acid, Nat. Geosci., 4, 440-443, doi: 10.1038/NGEO1164, 2011.